Article

Conception of High-Frequency Power Planar Transformer Prototypes Based on FabLab Platform

Simon Thomy, Xavier Margueron *, **Jean-Sylvio Ngoua Teu Magambo, Reda Bakri and Philippe Le Moigne**

Univ. Lille, Arts et Metiers Institute of Technology, Centrale Lille, Junia, ULR 2697 - L2EP, F-59000 Lille, France; simon.thomy@centralelille.fr (S.T.); jeansylvio@yahoo.fr (J.-S.N.T.M.); reda.bakri@centralelille.fr (R.B.); philippe.lemoigne@centralelille.fr (P.L.M.)

* Correspondence: xavier.margueron@centralelille.fr

Abstract: Conceiving planar magnetic components for power electronic converters is very constraining, especially in the case of prototype development. Indeed, such making requires skills, specific appliances as well as human time for setting up the machine tools and the fabrication process. With the emergence of Fabrication Laboratory (FabLab), conceiving of planar copper foil prototypes becomes more feasible in a shortened time process for engineers and researchers. This paper presents a methodology and process for conceiving power planar transformers with the help of machines and tools that can be found in the usual FabLab.

Keywords: HF planar transformer; fabrication laboratory; prototype manufacturing

1. Introduction

For some years now, planar transformers have gradually been replacing traditional high-frequency (HF) wounded transformers in embedded systems and electric vehicles. Planar components present many advantages like efficiency, power density, small size and less weight as well as good thermal characteristics [1–3].

Planar transformers are usually made of a printed circuit board (PCB) or copper foil windings combined with low profile magnetic core. Even if PCB windings present many advantages in terms of industrialization (manufacturability, cost reduction, repeatability), making multi-layer PCB transformer prototypes is complex and requires specific machines, technology and engineers' time. Planar component prototypes are then difficult to conceive, expensive and need to be subcontracted to specialists. This drawback was not as important when developing HF wounded transformers. For power planar components, copper foil can also be an interesting solution for a transformer's windings. Regarding prototypes, with such technology combined with the emergence of Fabrication Laboratory (FabLab) almost everywhere [4], making planar transformer prototypes becomes more feasible in an acceptable time, with a do-it-yourself (DIY) conception philosophy.

To address this issue, a complete conception process has been developed in order to achieve planar transformer prototypes. The process is suitable for any FabLab and creates opportunities to quickly elaborate affordable components. Therefore, this paper presents the complete process for the conception of planar transformer prototypes based on tools that can be found in FabLab. Based on electrical specifications, a planar transformer is designed, conceived in a FabLab and tested with specific power electronic equipment.

The paper is organized as follows: In Section 2, an introduction to the world of FabLabs is undertaken. In Section 3, technical considerations are listed dealing with the planar transformer design specificities. Then, a complete design of the planar transformer is performed based on models from the literature and finite element analysis (FEA). In Section 4, the full process to make a copper foil planar transformer prototype is described. The focus is on the key points and difficulties encountered in the prototype's development. In Section 5, the planar prototype is tested and characterized to validate its functioning. Finally, the process is discussed and potential improvements are highlighted.

2. FabLab

The first FabLabs were opened in the 2000s. These laboratories are dedicated to open-source creation, co-creation and local production [5] based on modern equipment and software. In 2016, 490 FabLabs were referenced in 72 countries [5]. In 2018, this number reached 650 in 80 countries [6] and it is still increasing quickly. That has led to a worldwide network of fabrication laboratories where almost everything can be made everywhere [4]. FabLabs are made for prototyping, making, learning, meeting and contributing to the maker community [7]. A lot of universities have created their own FabLab to form a new generation of high-tech FabLab-oriented makers [8].

The emergence of FabLabs is linked to the development of new philosophy of conception as well as the growth of new practical tools such as 3-D printers; 3-D printing, also called additive manufacturing, consists of machines that are able to add material layer-by-layer to create an object from 3D CAD (computer aided design) models. This topical subject concerns a lot of application domains from micro-systems [9] to aerospace and automotive industries [10] as well as education [11]. In 2020, during the health crisis, the makers' community, FabLabs and 3D-printing have played an important role in manufacturing personal protective equipment and ventilator replacement parts that could not be satisfied by regular suppliers [12–14]. Regarding power electronics, 3-D printing technology is now applied to magnetics, dealing with 3-D printed air-core inductors [15], low power planar inductors [16], shaped profile windings [17], cool fins for planar inductors [18] and wireless power transfer system [19].

The FabLab (Figure 1) involved in this study hosts a laser-cutter, four types of 3-D printers, a milling machine, wood-cutter, embroiderer, sewing machine and other more classical tools that can be found in electronic labs and workshop manufacturing.

Figure 1. FabLab "Make" at Centrale Lille Institut.

3. Technological Considerations for the High-Frequency (HF) Planar Transformer Prototype

3.1. Conceiving Planar Transformer: Printed Circuit Board (PCB) vs. Copper Foil

Planar transformer windings can be made with PCB (rigid or flex technology), copper foil and more rarely with Litz wires [20–25]. PCB technology is the most widespread, offering many advantages like mass production, repeatability, reliability or low leakage inductance [26]. PCB planar transformers can be connected as stand-alone or embedded

within a PCB-assembled converter to save space [27] or to increase power integration. On the other hand, the main drawback of PCB planar transformers is their parasitic capacitances [23] that can cause electro-magnetic interference (EMI) problems. Other limits deal with costs, especially in the case of prototypes, and technological limitations linked to the manufacturing capabilities.

With PCB technology, copper tracks are a real issue. Indeed, PCB copper thicknesses are limited to standard values: 17.5 µm, 35 µm, 70 µm, 105 µm, 210 µm and 435 µm. Due to these small values, paralleling layers is necessary to carry power electronic high current values. As a consequence, vias are needed to connect different layers of the same winding. Connections between layers is a known problem for multi-layer PCB. It can increase cost as well as track's equivalent resistance and can lead to hot spots, especially in HF.

PCB Flex technology is a solution to reduce vias in windings. A Flex PCB is adequate for 3D power electronics [28]. Even if it is more suitable for medium series and prototypes than traditional multi-layer PCB, Flex PCB copper tracks are not optimal in the case of HF power electronic magnetic components [21,22]. Such windings are more dedicated to low power HF transformers or specific devices like bendable transformers [29].

Regarding leakage inductances, distance between PCB layers and interleaving for reducing HF copper losses are factors that limit the leakage inductance values [26]. For some converters operating in soft-switching, it is interesting to increase the leakage value of a transformer to avoid the use of an additional inductance [30]. With a planar PCB transformer, this increase is limited due to PCB technological constraints and traditional available cores.

For an HF power planar transformer, copper foil windings appear like an interesting alternative to PCB windings. Some benefits can be highlighted:

- Copper track thicknesses are not limited. Bigger conductors can be selected in order to limit or at least reduce complex paralleling layers with respect to skin depth that is problematic. Moreover, primary and secondary thicknesses can easily be set to different values.
- Distance between layers can also be set to different values, stacking insulated layers. Insulation material can also be chosen differently according to layers.
- Leakage values can be increased by spacing primary and secondary windings or by introducing ferrite polymer composite (FPC) material between layers, like C350 for example [31].

As a major drawback, connections between layers need to be well thought out in the design step.

3.2. Transformer Prototype Specifications

The planar transformer developed in this study is defined for an aeronautic application for a More Electric Aircraft (MEA) [3]. It is designed for a 2 kW DC/DC Dual active bridge (DAB) power converter [32]. The circuit schematic is presented in Figure 2. The DAB electrical characteristics are listed in Table 1.
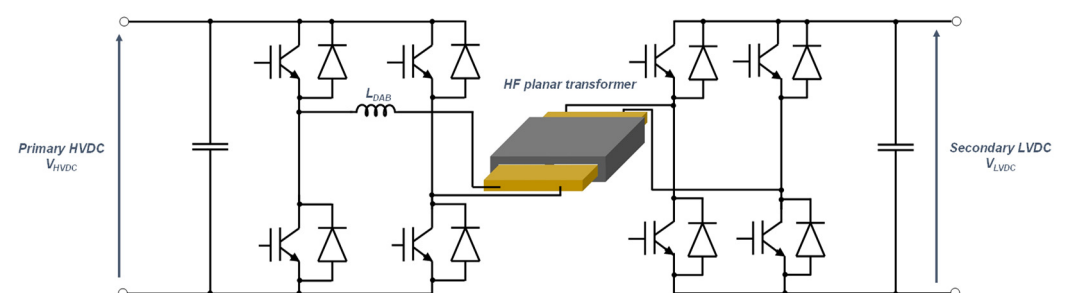

Figure 2. Dual active bridge (DAB) converter.

Table 1. Planar transformer electrical specifications.

Electrical Parameter	Value
Nominal Power	P_{nom} = 2 kW
Primary voltage (rms)	V_p = 400 V
Switching frequency	f_s = 100 kHz
Transformer ratio	η = 0.05
Magnetizing inductance	L_m = 0.5 mH

Due to the application, the prototype has to be lightweight. In terms of target design, a maximal temperature rise is fixed to ΔT = 120 °C, for a 20 °C ambient temperature and no cooling device (heat transfer by natural convection). The leakage inductance is not a key parameter for this design. Its value can be low. Indeed, an additional inductor is used to obtain the DAB maximal series inductance needed in transfer Function (1):

$$P_{out} = \frac{V_{HVDC}\, V_{LVDC}}{L_{DAB}\, f_s\, \eta}\, \varphi\left(\frac{\pi - |\varphi|}{2\pi^2}\right)$$ (1)

where φ is the phase shift between primary and secondary bridges, V_{HVDC} and V_{LVDC} are the voltages of the DAB converter (Figure 2) and L_{DAB} is the maximum allowable DAB inductance value set to 100 µH.

3.3. Transformer Design and Description

The magnetic core is selected based on the product area method [33]. With this method, the product A_p (2) of the window area A_w and the core cross-section A_c is expressed as a function of the power and other electrical specifications:

$$A_p = A_w A_c = \frac{P_{max}}{K_f K_r B_m f_s J_w}$$ (2)

where P_{max} is the maximal power, K_f is the waveform coefficient, K_r is the window filling factor, B_m is the flux density, f_s is the switching frequency and J_w is the current density.

Based on design specifications given in [3], the needed product area is calculated: A_p = 54,000 mm^4. The magnetic core, association of an E-shape E64 with a plate PLT64 [34], is selected according to this value. Indeed, the combination of both have a product area value of 57,600 mm^4. 3C90 ferrite material is selected.

Regarding windings, limitation of leakage inductance and copper loss lead to a solution with a complete interleaving between primary and secondary layers. Then, the windings are divided on 9 conductive layers of copper foils (Figure 3a). Number of turns for the primary is set to N_p = 20: four layers with five turns connected in series. The secondary contains only one turn (N_s = 1): five layers of one turn connected in parallel. Thus, the transformer ratio is 0.05. Primary and secondary layer thicknesses are set differently: 200 µm for the primary and 350 µm for the secondary. As mentioned before, such thicknesses are difficult to realize with PCB technology while keeping constant insulation layer thickness. Primary and secondary track widths are set to fulfill the current density requirement.

Dimensions and positioning of windings are presented in Figure 3a. Figure 3b shows a complete 3-D FEA Model made with ANSYS Maxwell 3D [35]. On these figures, insulation Kapton sheets between layers are not represented.

Magnetizing inductance is adjusted considering a 225 µm gap between the three legs of the planar E core and the plate one. With this gap value, the magnetizing inductance (3) should be of 0.53 mH:

$$L_m = A_L N_p^2$$ (3)

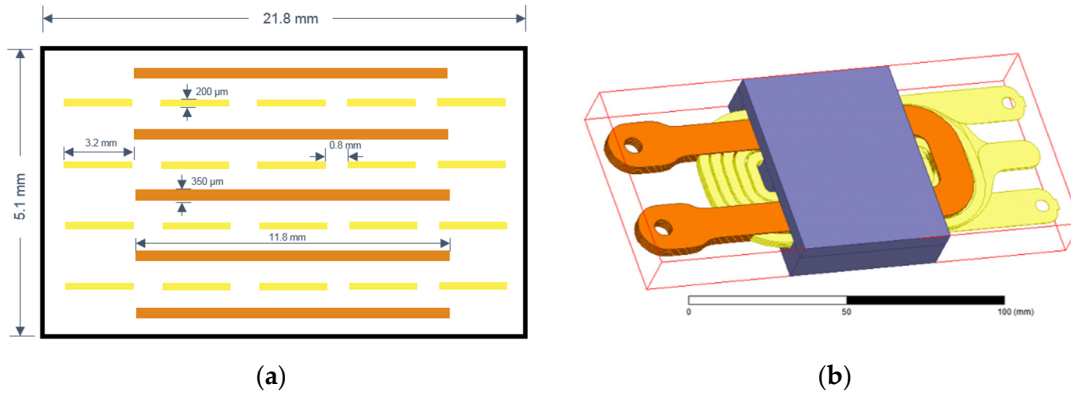where N_p is the primary turn number and A_L is the inductance factor of the ferrite core.

Figure 3. Planar prototype: (**a**) transformer's window; (**b**) three-dimensional finite element analysis (3-D FEA) model.

Leakage inductance is calculated with the model detailed in [36]. The estimated value from the primary winding is L_{lk} = 4.45 µH.

In a HF transformer, the general formula for calculating the copper losses in a winding is:

$$P_{Cu} = R_{DC} \times I_{DC}^2 + \sum_{n=1}^{\infty} R_{AC}(nf_s) \times I_{rms}^2(nf_s) \tag{4}$$

where R_{DC} is the DC resistance, I_{DC} is the DC current, R_{AC} is the AC resistance depending on frequency, I_{rms} is the rms value of each current harmonic and n is the harmonic order.

In the design example, the DC part of the current is null. R_{AC} is estimated based on Dowell model [37] for the primary winding and Ferreira [38] for the secondary winding. Both applied models are different for the primary and the secondary due to the difference of winding porosity factors. For the primary, the latter is estimated at 0.73 while for the secondary it is 0.51. Considering the current fundamental and the first four harmonics (3rd, 5th, 7th and 9th), copper losses are estimated to 21.1 W. As a comparison, the copper losses due to the current fundamental only are 20.3 W.

Core losses are calculated with the Mulder model [39] at ambient temperature:

$$P_f = k \times f_s^\alpha \times \hat{B}^\beta \times \left(c_{t0} - c_{t1} \times T + c_{t2} \times T^2 \right) \tag{5}$$

where k, α, β, c_{t0}, c_{t1} and c_{t2} are parameters for the magnetic material [39], $\hat{B}$ is the peak flux density and T is the temperature.

With this formula, for an ambient temperature of 25 °C and a peak flux density of 100 mT, the core losses are 4.84 W. This calculation corresponds to the worst case for core losses. Soft ferrite materials are usually optimized to have low losses between 80 °C and 100 °C.

In [40], McLyman gives an expression for the calculation of temperature rise in magnetics:

$$\Delta T = 450 \left(\frac{P_\Sigma}{A_t} \right)^{0.826} \tag{6}$$

where ΔT is the temperature rise, A_t is the effective surface area in cm^2 and P_Σ is the total dissipated power.

Based on (6), the thermal resistance of the transformer becomes:

$$R_{th} = \frac{450}{P_\Sigma^{0.174}} \left(\frac{1}{A_t} \right)^{0.826} \tag{7}$$

Finally, copper and core loss values lead to an estimated increased temperature ΔT = 106.1 °C with a thermal resistance R_{th} = 4.09 °C/W for the E/PLT64 planar core.

4. Prototype Achievement in FabLab Environment

Based on the FabLab platform, the prototype described in the previous section is now developed. After the process overview, each step is detailed, highlighting difficulties and precautions that have to be taken to obtain good and functional transformer.

4.1. Manufacturing Process Overview

Figure 4 presents the process overview, introducing all the equipment that has to be used. Firstly, all the elements are modeled using Onshape Software [41]. Then, the numerical files are transferred to specific tools that allow the different transformer's parts to be made: copper windings for primary and secondary units, insulating Kapton and add-ons for the assembling parts. Finally, all these elements are assembled together on a planar magnetic core.
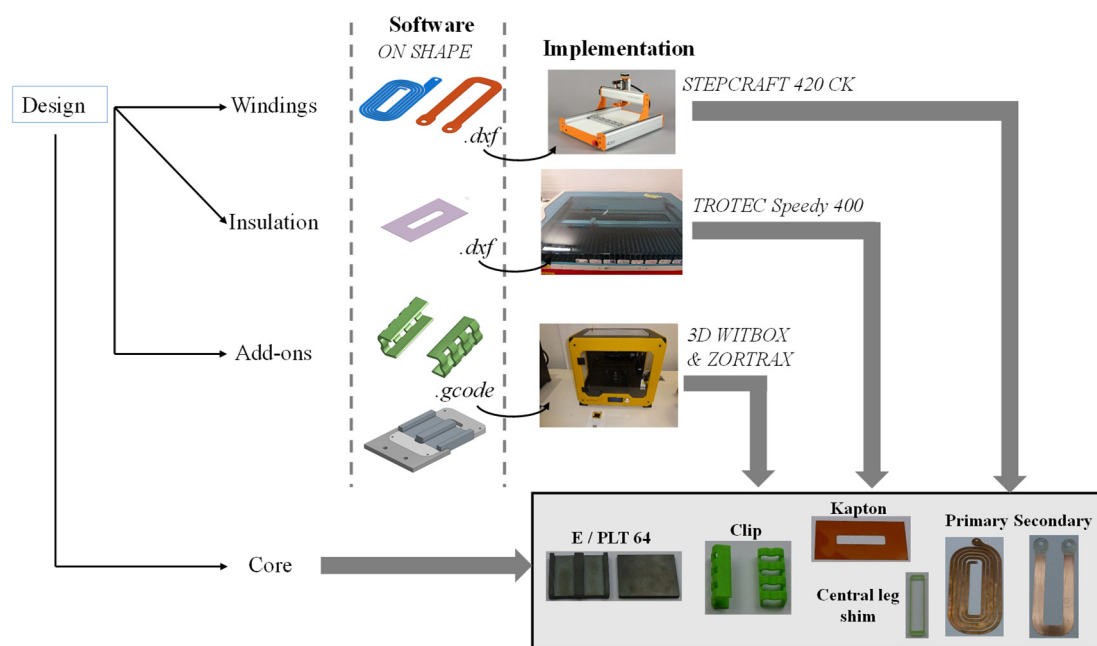

Figure 4. Process overview.

4.2. Parts Production

Three steps can be differentiated for the manufacturing of the different planar transformer's parts:

1. Copper windings: after their shape design, primary and secondary winding copper tracks are carved using a computer numerical control (CNC) machine Stepcraft 420 CK [42]. Figure 5 shows the milling process for two primary layers. During this process, lubricant is sprayed regularly. This provides two benefits: the drill run cooler and copper filings do not hang up. As a consequence, the drill's lifetime is extended. Then, endpoints of copper tracks are tined to ease connections between layers. Finally, winding layers are ready for assembling. One can note that all the secondary tracks are identical due to the parallel winding. On the opposite, primary layers are different in order to make possible series connections between the layers.

2. Kapton insulation: insulation between layers is made with Kapton film. Elementary 75 μm Kapton layers are then cut using the laser cutting machine Trotec Speedy 400 [43] to consider magnetic core and central leg size. Distances between winding layers will be set adding more or less of these elementary layers.

3. Add-ons: in order to assemble the transformer prototype, some supplementary elements have to be developed. Firstly, plexiglass clamps and secondary winding centering pins have to be cut with the laser cutting machine. All these elements are

made of polymethyl methacrylate (PMMA) material. Secondly, clips and central leg shim are printed in 3-D [44]. They are made of polylactic acid (PLA) material. Clips are used for maintaining both magnetic core parts together while the central leg shim is used for centering and spacing primary winding from the central core leg.
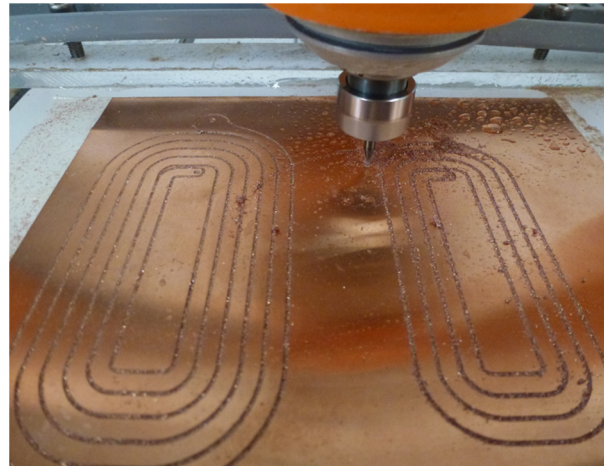

Figure 5. Milling windings.

4.3. Assembly Operations

Once all the parts have been made, everything is assembled layer by layer (Figure 6).

- Step 1: The plinth, including bottom clamps and centering pins is set around the E-part core.
- Step 2: Kapton insulated layers are added. Insulating thickness is adjusted adding more or less elementary layers.
- Step 3: First secondary layer is positioned using centering pins.
- Step 4: Kapton layers are added.
- Step 5: First primary winding is added. As can be seen in Figure 6, primary pins are located on the opposite side of the secondary winding. The biggest one corresponds to the winding connecting pin, while the smallest one, located close to the ferrite core, is used for connecting this layer to the next one. The primary winding's centering is ensured by the central leg shim that locks its positioning.
- Step 6: Stacking takes place, interleaving insulating layers, secondary winding layers and primary layers, respecting the layout introduced in Figure 3a. During this step, primary winding layers have to be soldered for setting the 20 turns of the winding.
- Step 7: When the last secondary layer is added, the stacking is almost over. Some insulated layers are inserted before the magnetic core to be closed with the ferrite PLT core part. The air gap is tuned adding some Kapton between E and PLT core parts. Then, the upper side of the plexiglass clamps is screwed to the bottom one to fix layers' stack. Clips are tightened around the magnetic core while the plinth with centering pins is removed.

The obtained final prototype is presented in Figure 7. This 2 kW planar transformer prototype weigh 295 g in a volume lower than 0.1 L.

It could be interesting to compare the obtained transformer to components that can be found in the manufacturer's catalogue. This benchmark comparison is quite difficult to realize because an HF transformer is usually designed for specific electrical constraints and cooling systems. Then, the comparison must be made with the same characteristics to be suitable.
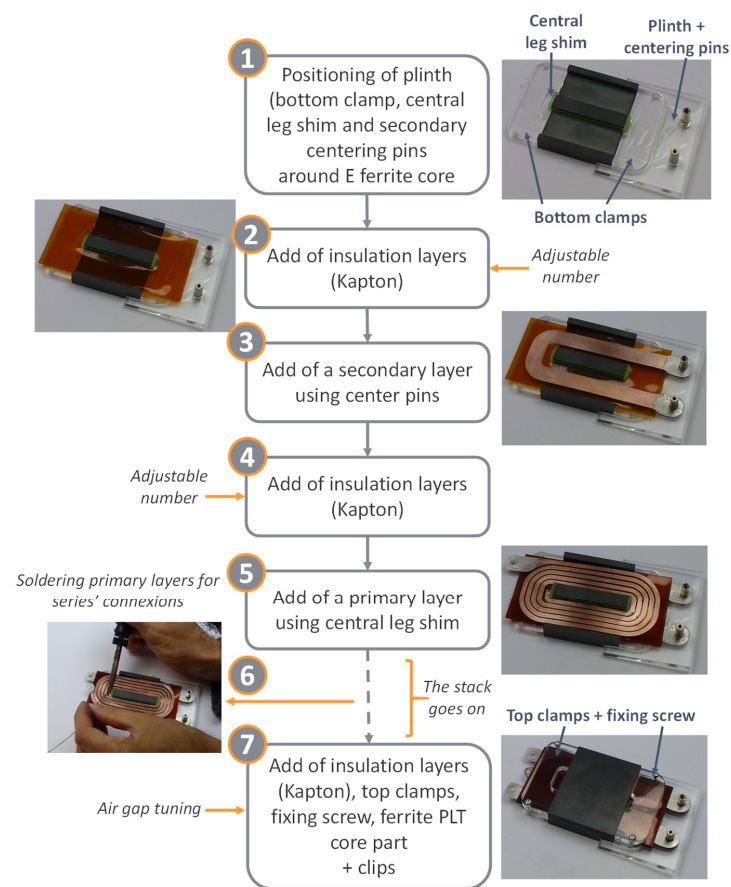
Figure 6. Assembling process layer by layer.

Figure 7. Planar transformer prototype.

In our case, the transformer is designed for use without a cooling system (heat transfer by natural convection). As a consequence, volume and weight of the prototype are higher

than another transformer with the same power, voltage, frequency and cooling system. However, in general, the manufacturer Payton gives a 10 to 15 g per 100 W [45] for their planar transformer. In this case, the developed prototype is consistent with their components.

5. Prototype Validation: Characterization and Tests

In this section, the prototype is characterized and tested in order to validate its good functioning.

5.1. Small Signal Characterization Based on Impedance Measurements

The characterization is performed with impedance analyzer HP4294A [46]. The four measurements with open and short circuits are shown in Figure 8. The obtained impedances are typical for an HF transformer. This first characterization step enables us to conclude that the prototype is working as a transformer. The equivalent circuit parameters (Figure 9) are extracted from these measurements [47]. It can be noted that the parasitic capacitive effect is not shown in Figure 9. Table 2 compares some parameter measured values to the theoretical ones. For a better accuracy, the DC resistances are measured with a micro-ohmmeter CA 6250 [48].
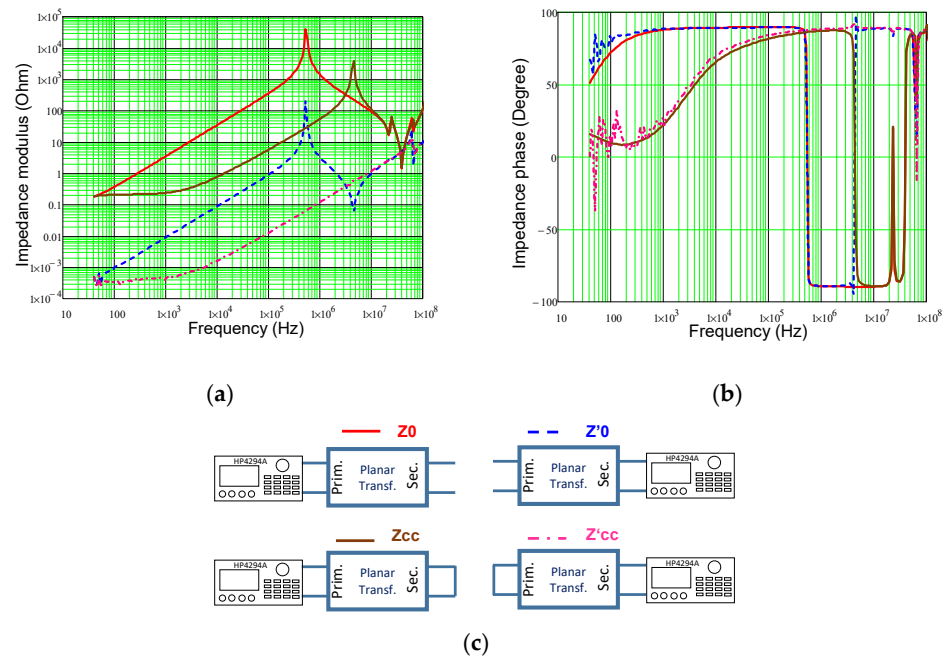

Figure 8. Planar transformer impedance measurements: (**a**) modulus; (**b**) phase; (**c**) measurement configurations.

These measurements are consistent with the theoretical ones, except for the low frequency leakage inductance seen from the primary winding. Indeed, the theoretical value, calculated with [36], is L_{lk} = 4.45 µH while the measured on is L_{lk_meas} = 16 µH. This difference can be explained by the short circuit (Figure 10a) used in the characterization process [49]. Regarding secondary impedance order of magnitude, the 3.2 cm short circuit copper conductor adds about 32 nH, i.e., 10 nH per centimeter, to the secondary leakage inductance. Subtracting this value (L_{sc}) from the measured primary value leads to consistent low frequency leakage value:

$$L_{lk\_LF} = L_{lk\_meas} - L_{sc} = 16 \cdot 10^{-6} - 32 \cdot 10^{-9} \cdot \frac{1}{\eta_{ps}^2} = 3.2 \text{ µH} \qquad (8)$$

This lack of precision also could be attributed to the manual assembling process that prevent a precise positioning of the layers.
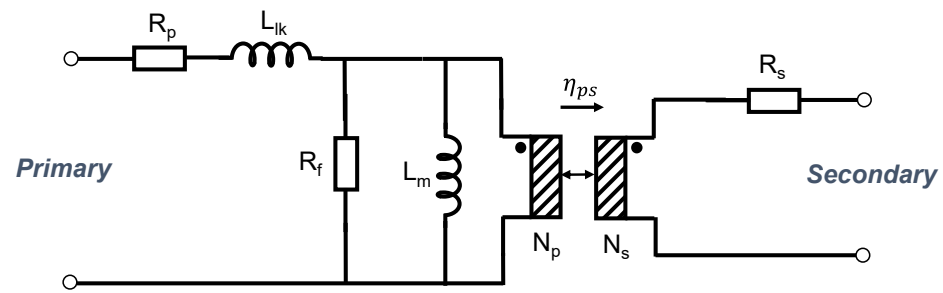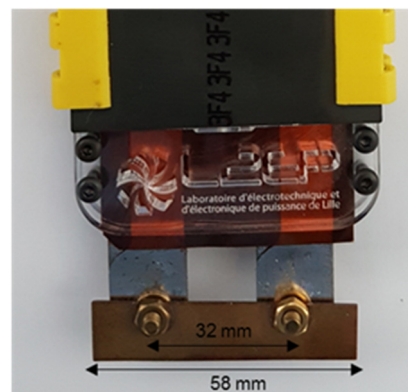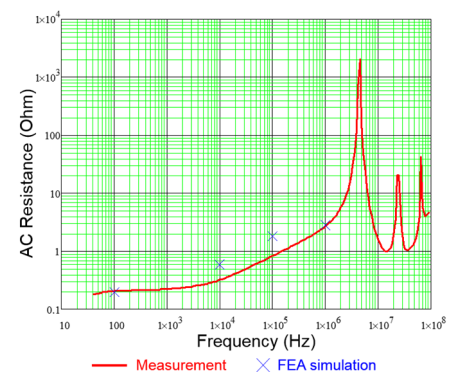
Figure 9. Planar transformer equivalent circuit.

Table 2. Planar transformer electrical characteristics.

Parameter	Symbol	Unit	Experimental Value	Theoretical Value
Transformer ratio	η_{ps}		0.05	0.05
Magnetizing inductance	L_m	mH	0.56	0.53
Leakage inductance (low frequency)	L_{lk}	μH	16	4.45
Primary DC resistance	R_p	mΩ	111.8	105.6
Secondary DC resistance	R_s	mΩ	0.198	0.22

(**a**)　　　　　　　　　　　　　　　　　　　　　(**b**)

Figure 10. Planar transformer characterization: (**a**) short-circuit. (**b**) alternating current (AC) resistance vs. frequency.

The AC resistance is plotted versus frequency on Figure 10b. For frequency below 1 MHz, these measurements are consistent with FEA simulation performed with Ansys [35].

5.2. Thermal Characterization with Open and Short Circuit Power Measurements

Four power tests were performed for the thermal characterization of the transformer with a 100 kHz inverter. For each test, the temperature distribution is obtained with a thermal infra-red camera Fluke Ti95 [50]. Electrical waveforms are also presented.

5.2.1. Open Circuit Test

The primary planar transformer is supplied with a square voltage (±400 V) from full bridge inverter (Figure 11). Losses are mainly core ones and can be estimated to be 4.6 W. The temperature of the core is close to 43 °C for an ambient temperature of 23.3 °C.
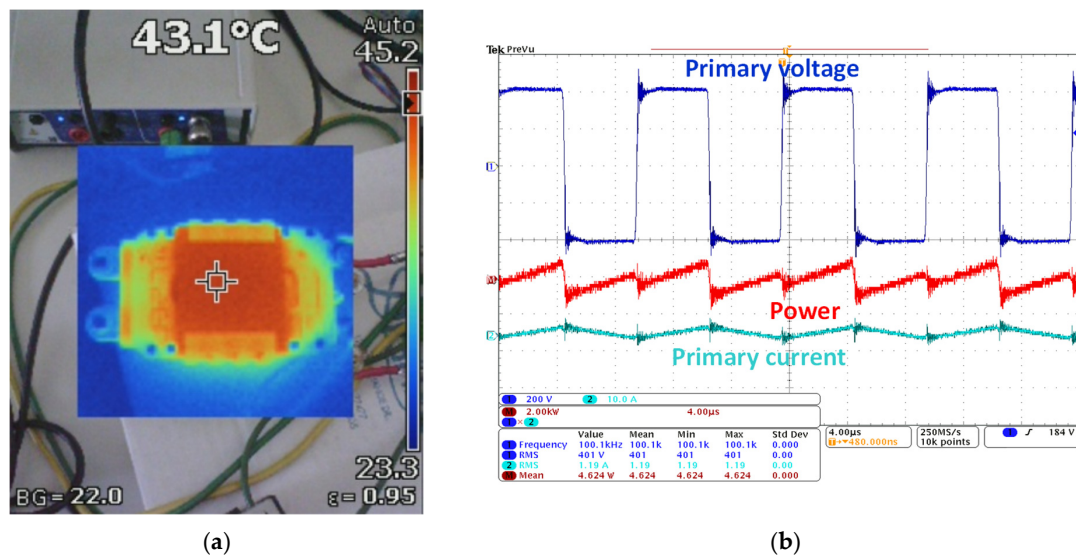
Figure 11. Thermal characterization—open circuit test: (**a**) temperature distribution; (**b**) voltage, current and power waveforms.

5.2.2. Short-Circuit Test

For this test (Figure 12), the voltage is reduced to 40 V. At the secondary winding, the current reaches 100 Arms. The measured losses, mainly copper ones, are 23.7 W. The temperature rise is 76.9 °C with an ambient temperature of 23.4 °C. On Figure 12a, one can note hot spots close to secondary terminations. Due to the current value and the parallel secondary layers, specific attention must be paid to this winding. Termination soldering must be done with a highly conductive material in order to solve this issue.
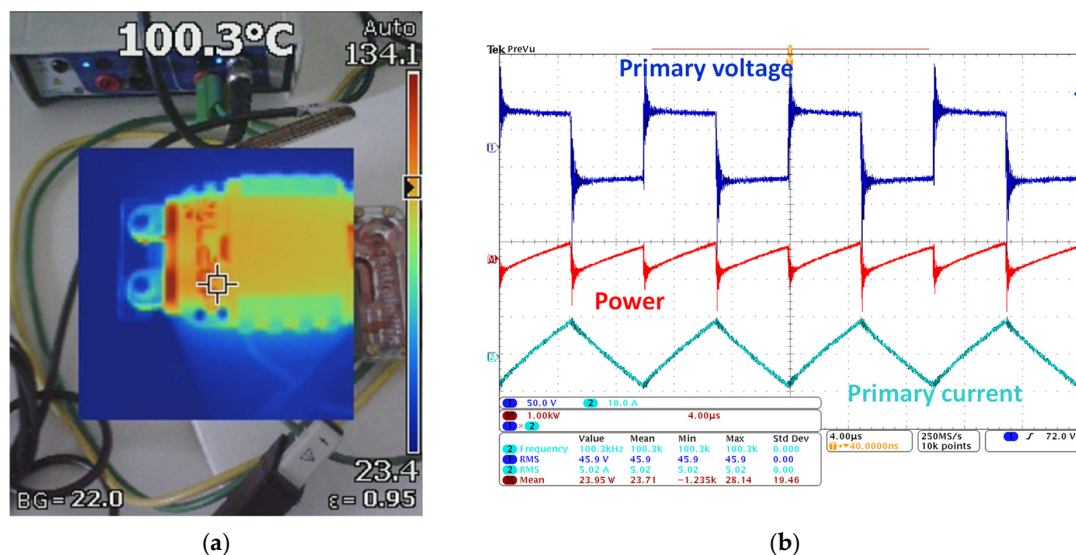
Figure 12. Thermal characterization—short-circuit test: (**a**) temperature distribution; (**b**) voltage, current and power waveforms.

5.2.3. Load Tests

Two load tests were finally performed. For these tests, the output of the planar transformer is connected to a rectifier and a variable resistor.

The first load test (Figure 13) is performed with a 1 kW resistive load. The primary rms voltage is 350 V while the secondary current is 53.9 A. The obtained temperature is 59.6 °C for 21.4 °C ambient temperature. Despite the load being half the nominal power,

the low temperature rise confirms the transformer capability to transfer power beyond 1 kW in natural convection.

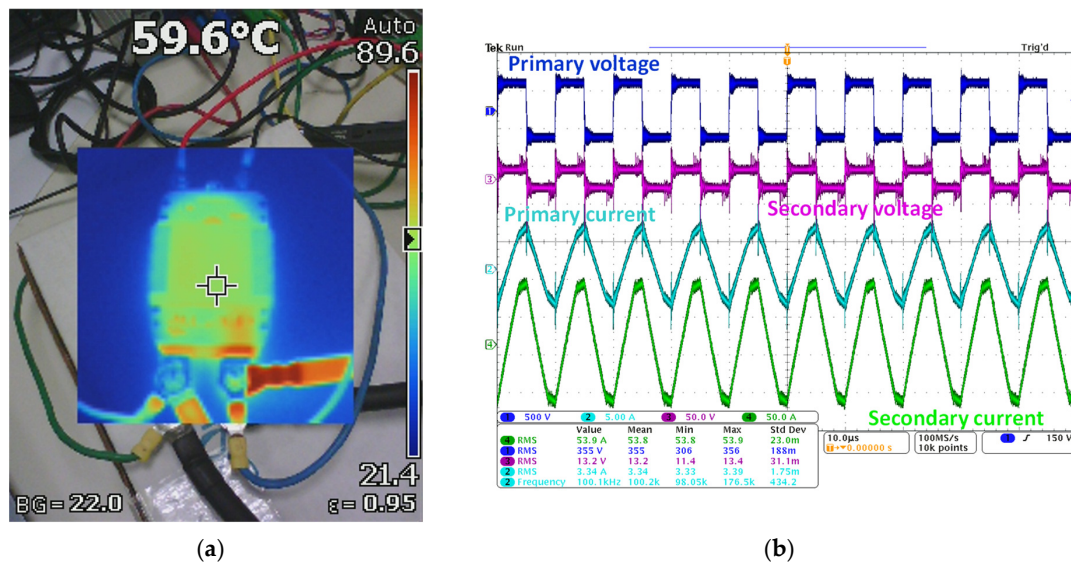(**a**)   (**b**)

Figure 13. Thermal characterization—350 V (primary)/53.9 A (secondary): (**a**) temperature distribution; (**b**) voltage and current waveforms.

The second load test (Figure 14) is performed with a resistive load closed to nominal power. The primary rms voltage is 400 V while the secondary current is 90.4 A. The temperature obtained is 121.7 °C for 23.9 °C ambient temperature. The temperature rise confirms the transformer capability to transfer this power. This result is consistent with the temperature rise computed in the Section 3.3. However, two comments can be made: firstly, the measured temperature with thermal infra-red camera is questionable and not so accurate, in particular for the winding temperatures. The use of thermo-couples could enable more accurate measurements to be made. Secondly, with such temperature, it would be necessary to use a fan to ensure normal operation for steady state uses. Such a cooling system will increase the lifetime of the transformer.

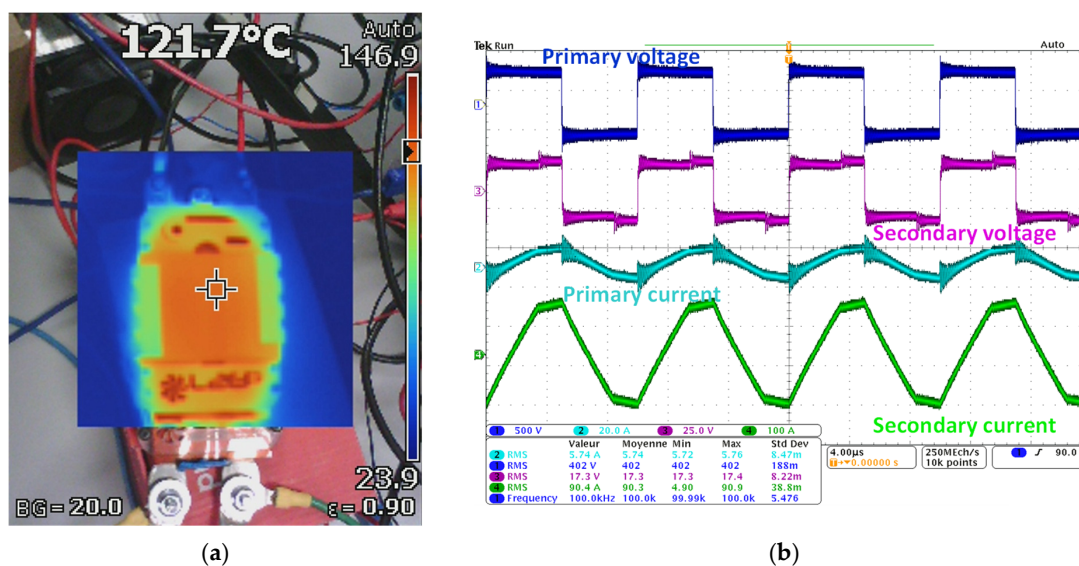(**a**)   (**b**)

Figure 14. Thermal characterization—400 V (primary)/90.4 A (secondary): (**a**) temperature distribution; (**b**) voltage and current waveforms.

5.3. Comments on Measurements and Process

The measurement results show that the design transformer is operational. Its parameters are closed to those estimated with analytical calculations and FEA modeling. Nevertheless, the leakage inductance theoretical value is too far from the measurement. This parameter must be investigated. This lack of precision could be attributed, in part, to the manual assembling process that prevent form a precise positioning of the layers. However, as mentioned in [49], this difference can also be attributed to the characterization process that must be revised. With such a step-down transformer with high current values at the output, precise measurements make it difficult to characterize secondary windings.

The described FabLab process has led to a functional planar transformer copper foil prototype. Compared to the multilayer PCB planar transformer technology, such a prototype presents benefits such as less complexity in a winding's connections, different and bigger copper layer thickness, and more tunable distance between windings as well as the potential add-on of FPC magnetic layer.

The prototype has been developed using only tools and machines that can be found in a traditional FabLab. With such an approach, making planar transformer becomes affordable for quite everybody, without recourse to complex, expensive and specific PCB multilayer machines. Of course, one can note that the process is only dedicated to power prototypes. Indeed, with lower power range, PCB solutions are acceptable and more realizable in a laboratory. Moreover, process time for each step of conception is not negligible and does not fill with a medium series production. For automated mass production, power planar transformers made of multilayer PCB remain the most attractive solution.

Regarding methodology improvements, insulated layers could be stuck to improve mechanical strength. This requires glue that tolerates functioning temperatures with a good coefficient of thermal expansion. Some good thermal conductor material could also be added in the windings to enhance thermal behavior of the power planar transformer.

At this stage, it might be interesting to investigate the aging of such planar transformer as in [51]. Indeed, copper windings and Kapton insulation can be subject to hot spot, as shown in Figures 13 and 14, that can affect the reliability and the lifetime of the planar transformer. The ecological impact of such a transformer could also be considered performing an eco-dimensioning study. Results could be compared to a planar PCB based technology ecological impact [52].

6. Conclusions

In this paper, the process for conceiving HF power planar transformer prototype with copper foil is described step by step based on machines and tools that can be found in a FabLab. Each elementary layer (copper windings, insulating Kapton) as well as add-ons are first realized independently before being stacked and assembled together. The focus is on difficulties and tricks that enable a functional planar transformer to be realized. A 2 kW planar transformer prototype is designed, developed and characterized with an impedance analyzer. Thermal measurements are also made with a HF power full bridge converter. The method and results are then discussed to highlight the limits of and improvements to the proposed process.

Author Contributions: Conceptualization, S.T., J.-S.N.T.M. and R.B.; methodology, S.T., J.-S.N.T.M. and R.B.; validation, X.M., J.-S.N.T.M. and R.B.; investigation, X.M., J.-S.N.T.M. and R.B.; writing—original draft preparation, X.M.; writing—review and editing, S.T., X.M., J.-S.N.T.M., R.B.; project administration, X.M. and P.L.M. All authors have read and agreed to the published version of the manuscript.

Institutional Review Board Statement: Not applicable.

Informed Consent Statement: Not applicable.

Data Availability Statement: The data presented in the study are available in the article.

Conflicts of Interest: The authors declare no conflict of interest.

References

1. Quirke, M.T.; Barrett, J.J.; Hayes, M. Planar magnetic component technology-a review. *IEEE Trans.Compon. Hybrids Manuf. Technol.* **1992**, *15*, 884–892. [CrossRef]
2. Ouyang, Z.; Andersen, M.A.E. Overview of Planar Magnetic Technology–Fundamental Properties. *IEEE Trans. Power Electron.* **2014**, *29*, 4888–4900. [CrossRef]
3. Ngoua, T.; Magambo, J.S.; Bakri, R.; Margueron, X.; Le Moigne, P.; Mahe, A.; Guguen, S.; Bensalah, T. Planar Magnetic Components in More Electric Aircraft: Review of Technology and Key Parameters for DC-DC Power Electronic Converter. *IEEE Trans. Transp. Electrif.* **2017**, *3*, 831–842. [CrossRef]
4. Betts, B. Bringing the factory home [Manufacturing Personal]. *Eng. Technol.* **2010**, *5*, 56–58. [CrossRef]
5. Redlich, T.; Buxbaum-Conradi, S.; Basmer-Birkenfeld, S.-V.; Moritz, M.; Krenz, P.; Osunyomi, B.D.; Wulfsberg, J.P.; Heubischl, S. OpenLabs—Open Source Microfactories Enhancing the FabLab Idea. In Proceedings of the 2016 49th Hawaii International Conference on System Sciences (HICSS), Koloa, HI, USA, 5–8 January 2016; pp. 707–715. [CrossRef]
6. Fiaidhi, J.; Mohammed, S. Fab Labs: A Platform for Innovation and Extreme Automation. *IT Prof.* **2018**, *20*, 83–90. [CrossRef]
7. Stephenson, M.K.; Dow, D.E. The community FabLab platform: Applications and implications in biomedical engineering. In Proceedings of the 2014 36th Annual International Conference of the IEEE Engineering in Medicine and Biology Society, Chicago, IL, USA, 26–30 August 2014; pp. 1821–1825. [CrossRef]
8. Angrisani, L.; Arpaia, P.; Bonavolonta, F.; Lo Moriello, R.S. Academic FabLabs for industry 4.0: Experience at University of Naples Federico II. *IEEE Instrum. Meas. Mag.* **2018**, *21*, 6–13. [CrossRef]
9. Gendreau, D.; Mohand-Ousaid, A.; Rougeot, P.; Rakotondrabe, M. 3D-Printing: A promising technology to design three-dimensional microsystems. In Proceedings of the 2016 International Conference on Manipulation, Automation and Robotics at Small Scales (MARSS), Paris, France, 18–22 July 2016; pp. 1–5. [CrossRef]
10. Lim, C.W.J.; Le, K.Q.; Lu, Q.; Wong, C.H. An Overview of 3-D Printing in Manufacturing, Aerospace, and Automotive Industries. *IEEE Potentials* **2016**, *35*, 18–22. [CrossRef]
11. Dahle, R.; Rasel, R. 3-D Printing as an Effective Educational Tool for MEMS Design and Fabrication. *IEEE Trans. Educ.* **2016**, *59*, 210–215. [CrossRef]
12. Fiorillo, L.; Leanza, T. Worldwide 3D Printers against the New Coronavirus. *Prosthesis* **2020**, *2*, 87–90. [CrossRef]
13. Tarfaoui, M.; Nachtane, M.; Goda, I.; Qureshi, Y.; Benyahia, H. 3D Printing to Support the Shortage in Personal Protective Equipment Caused by COVID-19 Pandemic. *Materials* **2020**, *13*, 3339. [CrossRef]
14. Rendeki, S.; Nagy, B.; Bene, M.; Pentek, A.; Toth, L.; Szanto, Z.; Told, R.; Maroti, P. An Overview on Personal Protective Equipment (PPE) Fabricated with Additive Manufacturing Technologies in the Era of COVID-19 Pandemic. *Polymers* **2020**, *12*, 2703. [CrossRef]
15. Liang, W.; Raymond, L.; Rivas, J. 3-D-Printed Air-Core Inductors for High-Frequency Power Converters. *IEEE Trans. Power Electron.* **2016**, *31*, 52–64. [CrossRef]
16. Yan, Y.; Ding, C.; Ngo, K.D.T.; Mei, Y.; Lu, G. Additive manufacturing of planar inductor for Power Electronics applications. In Proceedings of the 2016 International Symposium on 3D Power Electronics Integration and Manufacturing (3D-PEIM), Raleigh, NC, USA, 13–15 June 2016; pp. 1–16. [CrossRef]
17. Simpson, N.; Tighe, C.; Mellor, P. Design of High Performance Shaped Profile Windings for Additive Manufacture. In Proceedings of the 2019 IEEE Energy Conversion Congress and Exposition (ECCE), Baltimore, MD, USA, 29 September–3 October 2019; pp. 761–768. [CrossRef]
18. Yu, Z.; Yang, X.; Wei, G.; Wang, L.; Wang, K.; Chen, W.; Wei, J. A Novel High-Current Planar Inductor With Cooling Fins Based on 3-D Printing. *IEEE Trans. Power Electron.* **2021**, *36*, 12189–12195. [CrossRef]
19. Hou, T.; Xu, J.; Elkhuizen, W.S.; Wang, C.C.L.; Jiang, J.; Geraedts, J.M.P.; Song, Y. Design of 3D Wireless Power Transfer System Based on 3D Printed Electronics. *IEEE Access* **2019**, *7*, 94793–94805. [CrossRef]
20. Gunewardena, T.R. Manufacturing design considerations for planar magnetics. In Proceedings of the Electrical Insulation Conference and Electrical Manufacturing and Coil Winding Conference, Rosemont, IL, USA, 25 September 1997; pp. 309–311. [CrossRef]
21. Zumel, P.; Prieto, R.; Cobos, J.A.; Uceda, J. Comparative study of flex-foil technology in HF planar transformer windings. In Proceedings of the 2002 IEEE 33rd Annual IEEE Power Electronics Specialists Conference, Cairns, Australia, 23–27 June 2002; pp. 1248–1253. [CrossRef]
22. de Jong, E.C.W.; Ferreira, B.J.A.; Bauer, P. Toward the Next Level of PCB Usage in Power Electronic Converters. *IEEE Trans. Power Electron.* **2008**, *23*, 3151–3163. [CrossRef]
23. Saket, M.A.; Shafiei, N.; Ordonez, M. LLC Converters with Planar Transformers: Issues and Mitigation. *IEEE Trans. Power Electron.* **2017**, *32*, 4524–4542. [CrossRef]
24. Chen, M.; Araghchini, M.; Afridi, K.K.; Lang, J.H.; Sullivan, C.R.; Perreault, D.J. A Systematic Approach to Modeling Impedances and Current Distribution in Planar Magnetics. *IEEE Trans. Power Electron.* **2016**, *31*, 560–580. [CrossRef]

25. Wang, Y.; Roodenburg, B.; Haan, d.S.W.H. Comparative study of three transformer concepts for high current dual active bridge converters. In Proceedings of the 5th International Conference on Integrated Power Electronics Systems, Nuremberg, Germany, 11–13 March 2008; pp. 1–4.

26. Carsten, B.W. The low leakage inductance of planar transformers; fact or myth? In Proceedings of the APEC 2001, Sixteenth Annual IEEE Applied Power Electronics Conference and Exposition (Cat. No.01CH37181), Anaheim, CA, USA, 4–8 March 2001; pp. 1184–1188. [CrossRef]

27. Planar E Cores. Available online: https://elnamagnetics.com/wp-content/uploads/library/Ferroxcube-Documents/Planar_E_Cores.pdf (accessed on 10 October 2021).

28. Chen, C.; Huang, Z.; Chen, L.; Tan, Y.; Kang, Y.; Luo, F. Flexible PCB-Based 3-D Integrated SiC Half-Bridge Power Module With Three-Sided Cooling Using Ultralow Inductive Hybrid Packaging Structure. *IEEE Trans. Power Electron.* **2019**, *34*, 5579–5593. [CrossRef]

29. Ho, G.K.Y.; Zhang, C.; Pong, B.M.H.; Hui, S.Y.R. Modeling and Analysis of the Bendable Transformer. *IEEE Trans. Power Electron.* **2016**, *31*, 6450–6460. [CrossRef]

30. Tan, W.; Margueron, X.; Taylor, L.; Idir, N. Leakage Inductance Analytical Calculation for Planar Components with Leakage Layers. *IEEE Trans. Power Electron.* **2016**, *31*, 4462–4473. [CrossRef]

31. TDK. Available online: https://www.tdk-electronics.tdk.com/en (accessed on 30 November 2020).

32. Kheraluwala, M.N.; Gascoigne, R.W.; Divan, D.M.; Baumann, E.D. Performance characterization of a high-power dual active bridge DC-to-DC converter. *IEEE Trans. Ind. Appl.* **1992**, *28*, 1294–1301. [CrossRef]

33. McLymnan, C.W.T. Chapter 5 Transformer Design Trade-Offs. In *Transformer and Inductor Design Handbook*, 4th ed.; CRC Press: Boca Raton, FL, USA, 2011.

34. Ferroxcube. Available online: http://www.ferroxcube.com (accessed on 10 October 2021).

35. Ansys. Available online: http://www.ansys.com (accessed on 10 October 2021).

36. Margueron, X.; Besri, A.; Jeannin, P.; Keradec, J.; Parent, G. Complete Analytical Calculation of Static Leakage Parameters: A Step toward HF Transformer Optimization. *IEEE Trans. Ind. Appl.* **2010**, *46*, 1055–1063. [CrossRef]

37. Dowell, P.L. Effects of eddy currents in transformer windings. *Proc. Inst. Electr. Eng.* **1966**, *113*, 1387–1394. [CrossRef]

38. Ferreira, J.A. Improved analytical modeling of conductive losses in magnetic components. *IEEE Trans. Power Electron.* **1994**, *9*, 127–131. [CrossRef]

39. Design of Planar Power Transformer. Available online: http://ferroxcube.home.pl/appl/info/plandesi.pdf (accessed on 10 October 2021).

40. McLyman, C.W.T. Chapter 6 Transformer-Inductor Efficiency, Regulation, and Temperature Rise. In *Transformer and Inductor Design Handbook*, 4th ed.; CRC Press: Boca Raton, FL, USA, 2011.

41. Onshape. Available online: https://www.onshape.com/en/ (accessed on 10 October 2021).

42. Stepcraft. Available online: https://www.stepcraft-systems.com/ (accessed on 10 October 2021).

43. Trotec. Available online: https://www.troteclaser.com/en/ (accessed on 10 October 2021).

44. Zortrax. Available online: https://zortrax.com/ (accessed on 10 October 2021).

45. Payton. Available online: https://www.paytongroup.com/ (accessed on 23 November 2021).

46. Agilent 4294A Precision Impedance Analyzer. Available online: http://literature.cdn.keysight.com/litweb/pdf/04294-90060.pdf (accessed on 10 October 2021).

47. Margueron, X.; Keradec, J.P. Identifying the Magnetic Part of the Equivalent Circuit of n-Winding Transformers. *IEEE Trans. Instrum. Meas.* **2007**, *56*, 146–152. [CrossRef]

48. Chauvin Arnoux. Available online: https://catalog.chauvin-arnoux.co.uk/uk_en/c-a-6255.html (accessed on 10 October 2021).

49. Skutt, G.; Lee, F.C.; Ridley, R.; Nicol, D. Leakage inductance and termination effects in a high-power planar magnetic structure. In Proceedings of the 1994 IEEE Applied Power Electronics Conference and Exposition-ASPEC'94, Orlando, FL, USA, 13–17 February 1994; pp. 295–301. [CrossRef]

50. Ti95. Available online: https://www.myflukestore.com/ (accessed on 10 October 2021).

51. Shen, Z.; Wang, Q.; Wang, H. Degradation Analysis of Planar Magnetics. In Proceedings of the 2020 IEEE Applied Power Electronics Conference and Exposition (APEC), New Orleans, LA, USA, 15–19 March 2020; pp. 2687–2693. [CrossRef]

52. de Freitas Lima, G.; Rahmani, B.; Rio, M.; Lembeye, Y.; Crebier, J.-C. Eco-Dimensioning Approach for Planar Transformer in a Dual Active Bridge (DAB) Application. *Eng* **2021**, *2*, 544–561. [CrossRef]